SIN-CHN
SCIENTIFIC PRESS PTE.LTD.

Molecular & Cellular Biomechanics 2025, 22(1), 803.
https://doi.org/10.62617/mcb803

Article

Biomechanical study on adsorption properties of modified rice husk based activated carbon for sulfamethoxazole

Zixuan Li, Jiaenlisheng Kuermanaili, Xinyu Lu, Xiaomin Li*

Laboratory of Pollutant Chemistry and Environmental Remediation, School of Chemistry and Chemical Engineering, Yili Normal University, Yining 835000, China
*** Corresponding author:** Xiaomin Li, 3188558223@qq.com

CITATION

Li Z, Kuermanaili J, Lu X, Li X. Biomechanical study on adsorption properties of modified rice husk based activated carbon for sulfamethoxazole. Molecular & Cellular Biomechanics. 2025; 22(1): 803.
https://doi.org/10.62617/mcb803

ARTICLE INFO

Received: 14 November 2024
Accepted: 25 November 2024
Available online: 10 January 2025

Abstract: The use of waste desiliconized rice husk charcoal as the base material and modified activation treatment with potassium hydride and cobalt aric acid are aimed at preparing a nitrogen-doped magnetic activated carbon material, so as to explore and use the adsorption method to study its performance of sulfamethoxole. Incorporating biomechanical principles allows for a deeper understanding of how structural attributes influence adsorption efficiency. The effects of pH, initial dye concentration, time and temperature on the adsorption behavior of materials were studied. For example, pH can significantly alter the surface charge of the adsorbent, affecting electrostatic interactions with the antibiotic molecules. Temperature influences molecular motion, enhancing the likelihood of successful adsorption events. Fourier infrared Spectrometer (FI-IR), scanning electron microscope (SEM), BET, thermoweight (TG) and other equipment were used to analyze its characteristics. The experimental results showed that the adsorption effect was best when the mass ratio of activated rice husk charcoal to cobalt acetate and urea was 1:0.4:2, the specific surface area could reach 900.9527 $m^2 \cdot g^{-1}$, and the average pore size was 3.0412 nm. At an initial concentration of 100 $mg \cdot L^{-1}$, the dosage is 0.015 g, the temperature is 35 ℃, and the adsorption time is 240 min, the adsorption effect is the best. The optimal adsorption combination was as follows: dosage of 0.015 g, initial concentration of sulfamethoxazole 100 $mg \cdot L^{-1}$, the adsorption time was 240 min, and the maximum adsorption capacity could reach 100.04 $mg \cdot g^{-1}$, and the adsorbent dosage had the most significant effect on the adsorption effect. Through the adsorption isotherm fit process, it conforms to the Freundlich adsorption isotherm model and belongs to chemical adsorption. This research highlights the biomechanical interactions at play in the adsorption process, providing a foundation for developing effective strategies to address sulfonamide antibiotic contamination through advanced activated carbon materials.

Keywords: biochar; rice husk; sulfamethoxazole; adsorption; biomechanics
Classification number in the middle picture: O613.71
Document logo code: A

1. Preface

Rapid urbanization and industrialization have caused serious environmental problems, especially water pollution. It is estimated that about 300 million tonnes of micropollutants, including drugs, hormones, industrial chemicals, pesticides, and flame retardants, are discharged into natural water bodies through wastewater each year [1]. Many domestic and international studies have reported that a variety of antibiotics have been detected in natural water environments, including natural water bodies such as oceans, rivers, lakes, and groundwater [2]. Among these organic pollutants, pharmaceuticals have received widespread attention due to their toxicity

and non-biodegradability, as well as irreversible long-term side effects on aquatic organisms [3]. According to the existing literature, a variety of antibiotics have been detected in many rivers at home and abroad, with concentrations ranging from 0.13–1900 $ng \cdot L^{-1}$ [4]. Important rivers in China, such as the Yangtze River, the Yellow River, and the Pearl River, have all been detected with antibiotic pollutants [5]. Therefore, the removal of these pharmaceutical micropollutants from wastewater has become one of the most challenging issues, requiring the development of a sustainable, efficient, and flexible treatment method [6]. Biodegradation, electrochemical catalysis, ozone oxidation, coagulation and flocculation, and membrane filtration have been widely used to remove drugs from wastewater [7]. However, the complex structure of the drug, the formation of toxic by-products, and the high cost of operation or maintenance are the main drawbacks of these methods [8]. Compared with the above methods, the adsorption method has the advantages of economy, renewability, and operational flexibility, and is considered to be a promising method for removing various pollutants from wastewater [9].

As a broad-spectrum antibiotic, sulfamethoxazole plays an important role in the treatment of multiple infectious diseases [10]. Despite its high residual concentration in the natural environment, it is regrettable that the purification efficiency of sulfamethoxazole is much lower than other similar drugs, highlighting the urgency of exploring efficient purification methods [11]. As a mature and easy to operate pollution control strategy, adsorption technology has been widely proved to effectively fix and remove pollutants in water [12,13]. However, the large-scale application of this technology is often limited by high costs, so the development of cost-effective adsorption materials is the focus of current research. In this context, activated carbon and biomass char stand out as two common adsorption materials and have received wide attention [14].

Rice in Xinjiang is one of the key food crops [15]. It is widely planted in Qapqar County, Yili. However, the remaining rice husk after rice processing, as biomass waste, its traditional treatment methods, such as combustion or abandonment, have proved to cause direct pollution problems to the environment [16]. This unutilized resource—rice husk, is negatively affecting the living environment of human beings.

However, compared with other agricultural residues, rice husks have unique characteristics such as high silicon content, high porosity, light weight, and very large surface area, making them valuable materials for industrial applications. As a result, many factories process rice husks to extract the required silicon components to make desilicated rice husk charcoal. Rice husk charcoal is a natural material with the advantages of porous structure, large specific surface area, high chemical stability, and abundant active functional groups [17]. However, due to the limitation of its own properties, the adsorption capacity of rice husk charcoal for antibiotics is small, and the removal effect is not good. In order to solve this problem, it is necessary to modify rice husk charcoal to increase its specific surface area, thereby improving its adsorption performance [18].

Based on the above understanding, in this study, the desilicated rice husk char was activated to improve the adsorption capacity of biochar, and in addition, cobalt and nitrogen elements were co-doped on rice husk char to prepare magnetic activated

carbon to facilitate the re-recycling of biochar from water, and the adsorption capacity of activated carbon for sulfamethoxazole was further improved due to the doping of N elements.

2. Experimental part

2.1. Experimental materials, reagents, and instruments

Desilicate rice husk charcoal (Xinjiang Yili) potassium hydroxide (AR, fu Chen (Tianjin) chemical reagent co., LTD.), cobalt acetate (AR, fu Chen (Tianjin) chemical reagent co., LTD.), urea (AR, fu Chen (Tianjin) chemical reagent co., LTD.), absolute ethanol (AR, Shanghai aladin biochemical technology co., LTD.), sulfamethoxazole (AR, Shanghai aladin biochemical technology co., LTD.)

The solution absorbance was measured by V-1500PC visible spectrophotometer, QW-YC2102 for oscillation adsorption, SEM (SEM, ZEISS-Sigma-300) of different biochar surfaces by Fourier transform infrared spectrometer (FT-IR, WQF-530), and TG/DTG curve of the materials tested by thermal-weight analyzer (STA-449-F5, Germany NETZSCH).

2.2. Empirical method

2.2.1. Preparation of the metallic cobalt biochar

Weigh a certain amount of pretreatment after 100 mesh screen silicone rice husk charcoal, and according to the mass ratio of 1:3.5 and potassium hydroxide, adopt solid phase grinding method to make the full reaction, reaction complete biochar placed in the tubular furnace into nitrogen protection, 750 ℃ activation for 1 h, the active biochar (KC) washed with distilled water to neutral. For the preparation of 1 g of KC, 1.4 g of cobalt acetate, 10 mL of absolute ethanol and 10 mL of distilled water urea (1.3 g), the mixture in a 75 ℃ thermostatic water bath at 500 $r \cdot min^{-1}$ for 1 h. The above mixture was dried at 105 ℃ in a temperature oven, then placed in a tubular furnace for 800 ℃, 30 min, washed with distilled water to neutral and dried for reserve, called NCo-0.4-KC.

2.2.2. Adsorption test of sulfamethoxazole

For the experiment, a specific amount of adsorbent and concentration were selected and placed in a 250 mL conical bottle. The conical bottle was placed in a constant temperature oscillator for 25 ℃ oscillation (200 $r \cdot min^{-1}$) to be shaken, and the upper clear liquid was filtered with 0.45 um filter head. In the subsequent steps, sulfammexazole concentration was analyzed by spectrophotometry (λ =265 nm), and all measurements were carried out in three parallel tests.

2.2.3. Plots of the standard curve of sulfamethoxazole

The standard solution of sulfamethoxazole was diluted with 0.1 $mol \cdot L^{-1}$ NaOH to concentrations of 2, 3, 4, 5, 6, 7, 8, 9, 10, and 11 $mg \cdot L^{-1}$. The 0.1 $mol \cdot L^{-1}$ NaOH solution was a blank solution. The absorbance of the sulfamethoxazole solution was measured at 265 nm in a UV-visible spectrophotometer. Based on these data, a standard curve between the absorbance and the concentration was established: $y = 0.05188x + 0.00076$, $R^2 = 0.9998$ (**Figure 1**).

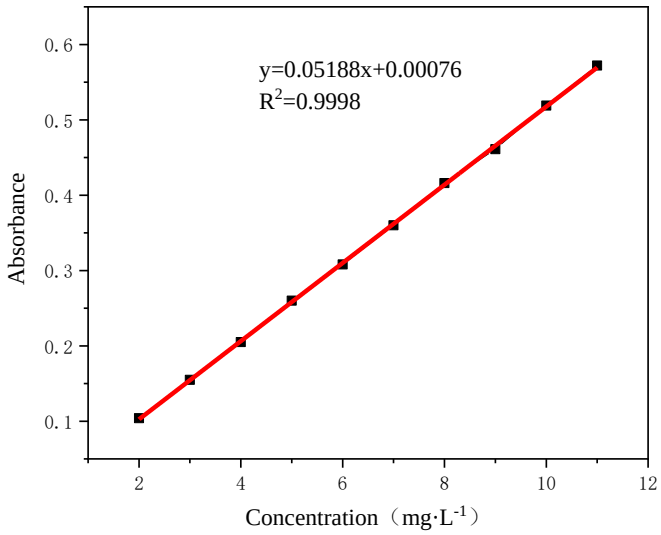

Figure 1. Sulfamethoxazole standard curve.

2.3. Related calculation formula

$$Q_e = \frac{(C_0 - C_e)V}{M} \tag{1}$$

$$E\ （\%）= \frac{（C_0 - C_e）}{C_0} \times 100\% \tag{2}$$

The linear expression of the quasi-first-order dynamics equation is:

$$ln\ （Q_e - Q_t) = ln\, Q_e - K_1 t \tag{3}$$

The linear expression of the quasi-second-order dynamics equation is given as follows:

$$\frac{t}{Q_t} = \frac{1}{K_2} \times \frac{1}{Q_{e^2}} + \frac{t}{Q_e} \tag{4}$$

Langmuir the adsorption of the isotherms:

$$\frac{C_e}{Q_e} = \frac{1}{K_L} \times \frac{1}{Q_m} + \frac{Q_e}{Q_m} \tag{5}$$

Freundlich the adsorption of the isotherms:

$$log\ Q_e = \frac{1}{n} log\ C_e + log\ K_F \tag{6}$$

where: The adsorption amount of Q_e-adsorbent at equilibrium is measured in: mg·g^{-1}

The initial concentration of C_0-sulfamethoxazole, in: mg·L^{-1}

The concentration of C_e-sulfamethoxazole at equilibrium is: mg·L^{-1}

Amount of *M*-adsorbent in: g

Concentration of the *V*-sulfamethoxazole solution in: L

E-Remorate of sulfamethoxazole in water by sorbent in: %

Q_t represents the amount of adsorption in t min: mg·g^{-1}

The *t* represents the adsorption time, in units of: min

K_1 indicates the quasi-first-order kinetic adsorption rate constant in units of: $g\cdot(mg\cdot min)^{-1}$

K_2 represents the quasitwo-quasikinetic adsorption rate constant in units: $g\cdot(mg\cdot min)^{-1}$

Q_m is the saturated adsorption amount, in units of: $mg\cdot g^{-1}$

K_L is the equilibrium constant, in units of: $L\cdot mg^{-1}$

And n and K_F are the Freundlich constant, in units of: $(mg\cdot g^{-1})(L\cdot mg)n^{-1}$

3. Results and analysis

3.1. Biochar characterization

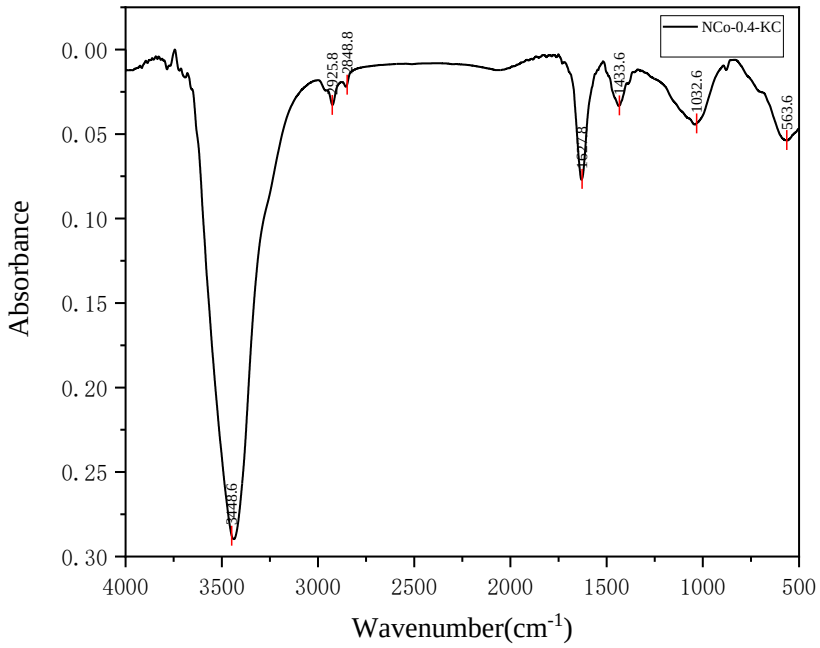

Figure 2. FT-IR spectra of NCo-0.4-KC biochar.

Figure 2 shows the infrared spectrum of the resulting NCo-0.4-KC biochar. Among them, the obvious broad absorption peak at 3438 cm^{-1} is the stretching vibration peak belonging to intermolecular hydrogen bond (O-H), at 2926 cm^{-1}, it can be inferred that the absorption peak is alkane (C-H) expansion vibration, and at 2948 cm^{-1}, it can be inferred that the absorption peak is methylene (CH_2-) expansion vibrationat 1697 cm^{-1}, this infrared spectrum characteristic peak is amide (C=N) vibration peak. The absorption peak at 1433 cm^{-1}) is inferred from the absorption peak amide (C-N). The characteristic peak at 1032 cm^{-1} is the expansion vibration of the ether characteristic absorption (C-O-C), which is due to the dehydration reaction. The absorption peak occurs at 563 cm^{-1} for the aromatics (C-H) surface.

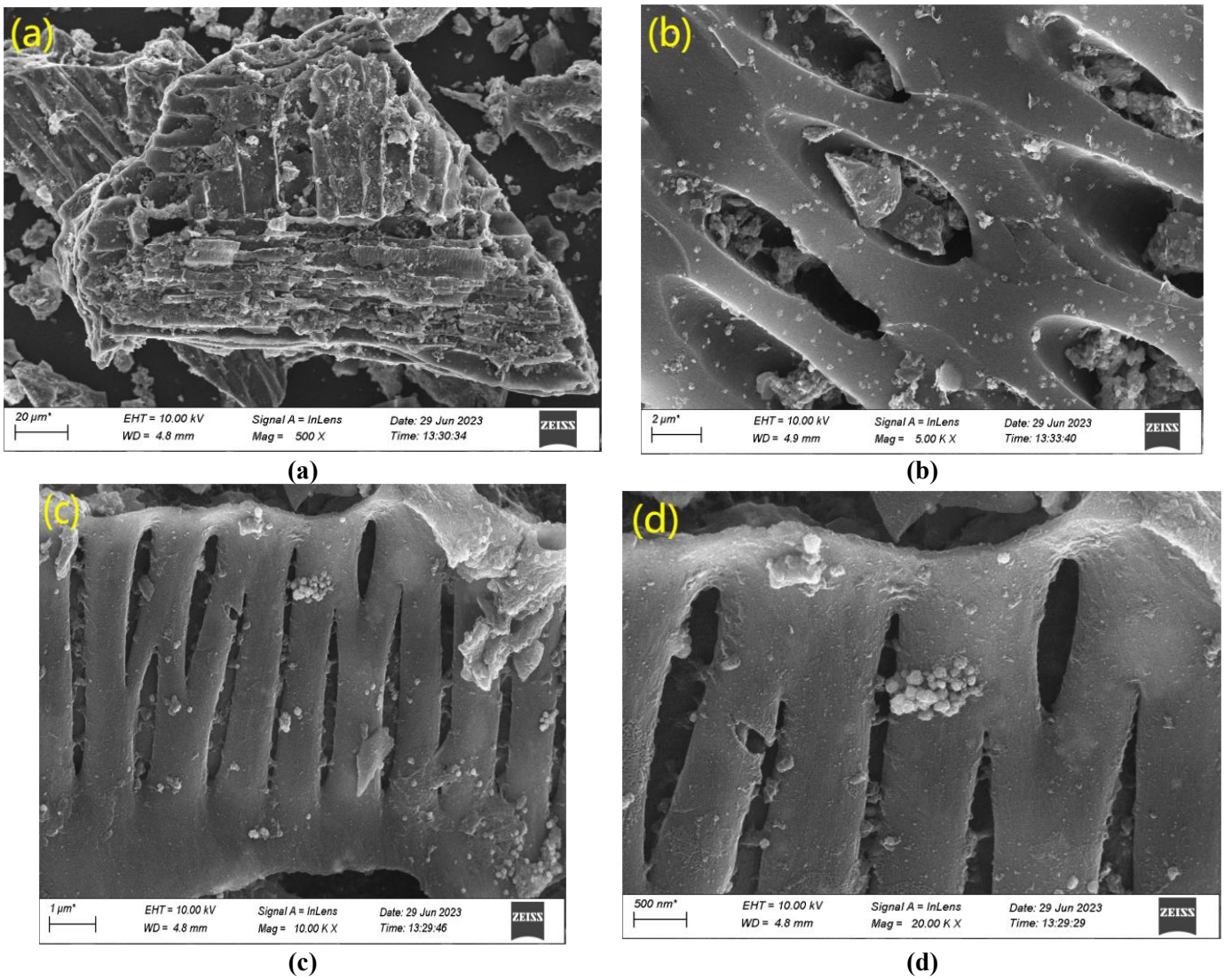

(a) **(b)** **(c)** **(d)**

Figure 3. (a), **(b)**, **(c)**, **(d)** are SEM images of NCo-0.4-KC.

Figure 3 presents the scanning electron microscopy (SEM) images of the NCo-0.4-KC biochar. Specifically, **Figure 3a** reveals the surface properties of NCo-0.4-KC biochar at 500 × magnification, which is locally rough and spread over deep valley structures, with significant lysis features leaping on the map. A further increase to 5000 times magnification, it was observed that the biochar surface is scattered with numerous mesoscopic scale holes, and these holes show a profound invagination structure. When the magnification is increased to 10,000 times, as shown in, spherical particles are widely distributed on the biochar surface, a phenomenon attributed to the incorporation of cobalt acetate leading to the dispersion of Co atoms on the biochar matrix. In addition, the presence of fine particles can be identified in the pores inside the biochar at up to 20,000 times. This finding not only confirms that the successful penetration of cobalt acetate into the microporous structure of the biochar, but also shows that the biochar has uniform pore size and good adsorption.

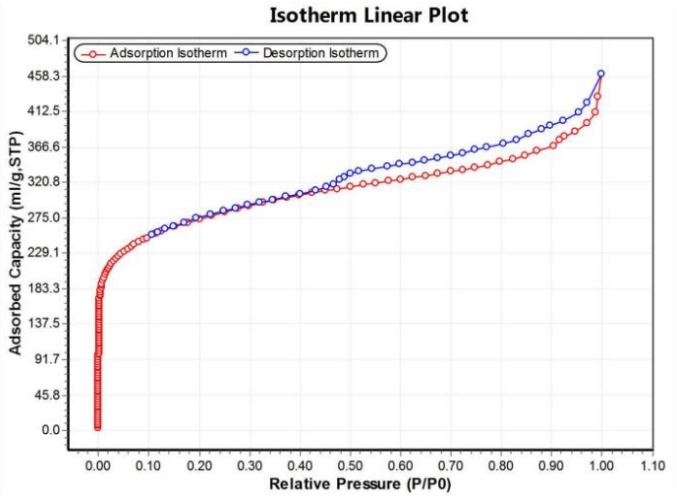

Figure 4. N_2 adsorption-desorption curves of NCo-0.4-KC.

The N_2 adsorption-desorption method was used to determine the specific surface area and pore size of NCo-0.4-KC biochar. As shown in **Figure 4**, the hysteresis loop of the NCo-0.4-KC adsorption isotherm is wide (P/P0 > 0.4), indicating that NCo-0.4-KC has a rich pore structure. It can also be seen that the NCo-0.4-KC adsorption-desorption curves conformed to the H_4-type hysteresis loop of the type IV isotherm [19], indicating that a large number of mesopores existed in NCo-0.4-KC, which was consistent with the pore-size information in **Table 1**, and these structural features enabled the NCo-0.4-KC adsorption TC process to proceed smoothly.

Table 1. Specific surface area and porosity of the samples.

Sample name	Specific surface area ($m^2 \cdot g^{-1}$)	Pore volume ($cm^3 \cdot g^{-1}$)	Average pore size (nm)
KC	259.6722	0.2692	4.1468
NCo-0.4-KC	900.9527	0.6850	3.0412

Figure 5 shows the TG/DTG curves of material NCo-0.4-KC, from which it is observed that NCo-0.4-KC has a high thermal stability. In the preheating phase, with the temperature below 100 ℃, NCo-0.4-KC lost only 7.33% of its mass, mainly due to the dehydration reaction of NCo-0.4-KC itself, and the dehydration process has a low temperature because water molecules are free to evaporate without proceeding within a specific temperature interval. Release of small molecules such as CO, CO_2 and H_2 were also observed. It is worth noting that NCo-0.4-KC exhibits minimal mass loss in a wide temperature domain of 100 ℃ to 800 ℃, which emphasizes that the material modified with cobalt acetate is significantly improved in high temperature resistance and structural stability compared to the unmodified KC biochar.

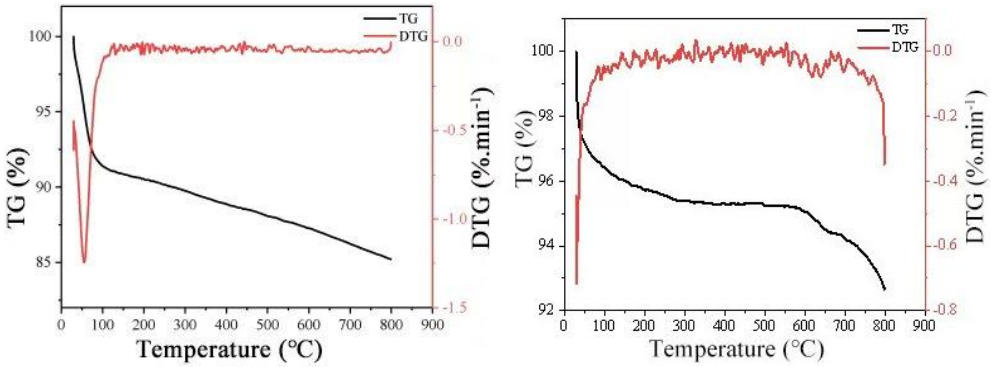

Figure 5. TG/DTG curve of KC and NCo-0.4-KC.

3.2. Effect of different mass ratios on the adsorption of sulfamethoxazole

Weigh 0.010 g of rice husk charcoal in different ratios, and configure with an initial concentration of 20, 40, 60, 80, 100, 120 and 140 mg·L^{-1}, sample in the full temperature shaker for 120 min, to determine the absorbance change at each concentration level. As can be seen from **Figure 6**, in the initial concentration range of 80 to 100 mg·L^{-1}, different proportions of carbon showed stronger adsorption capacity with increasing concentration [20]. However, the trend of this adsorption capacity leveled when concentrations exceeded 100 mg·L^{-1}. It shows that the available adsorption sites on the biochar surface are gradually saturated, leading to a significant slowdown in the adsorption rate [21]. Among them, the carbon with a mass ratio of 0.4:1 showed the maximum adsorption amount at the initial concentration of 100 mg·L^{-1}, reaching 138.78 mg·g^{-1}. Therefore, it can be judged that the 0.4:1 carbon has the best adsorption effect on sulfamethoxazole.

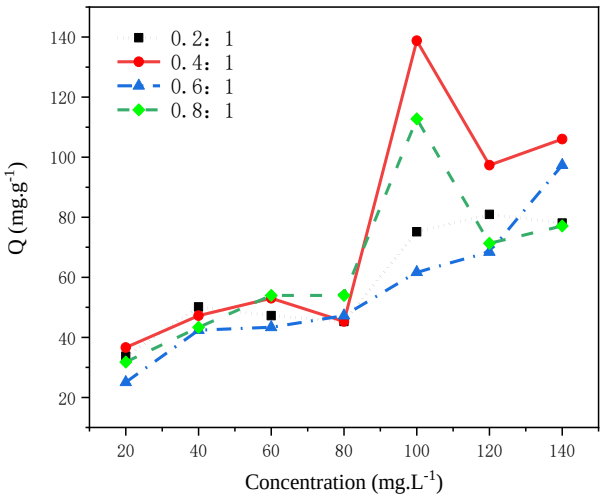

Figure 6. Effect of different mass ratios on the adsorption of sulfamethoxazole.

3.3. Effect of adsorption on the absorption of sulfamethoxazole at different times

To explore the optimal adsorption period of sulfamethoxazole, 0.010 g of adsorption material was used with a mass ratio of 0.4:1 and. The subsequently with

100 mg·L^{-1} concentration of sulfamethoxazole solutione. The entire experimental process was performed at 25 ℃ in a thermostatic shaker to ensure temperature stability in the experimental conditions. The sampling time points were carefully selected to cover multiple time nodes between 2 and 720 min, aiming to comprehensively capture the adsorption dynamics. Through this process, the data reveal the trend characteristics of the absorption amount of sulfamethoxazole and the removal efficiency to increase first and then decrease over time. According to the experimental results **Figure 7**, it can be observed that with the increase of time, the adsorption amount and removal rate of sulfamethoxazole showed a trend of rising first and then decreasing. At 240 min, the adsorption of sulfamethoxazole climbed to a peak of 94.45 mg·g^{-1}, and the removal rate reached 18.96%. Shows the optimal adsorption efficiency at this moment. It shows that the adsorption efficiency is optimal at this moment. After more than 240 min, the adsorption capacity and removal rate began to decrease gradually, but remained at a high level. This strongly proves that biomass activated carbon has excellent and durable adsorption capacity for sulfamethoxazole. From the perspective of adsorption dynamics, the process can be divided into three clear stages: the initial rapid adsorption, the subsequent slow growth and the final adsorption equilibrium achievement stage. In the initial stage of adsorption, the adsorption rate is extremely rapid due to the dual effect of the high drug concentration and the rich active site of the adsorption medium. With the time evolution, with the decrease of the drug concentration and the adsorption site, the adsorption rate slows down until the equilibrium state is established, and both the adsorption rate and removal rate reach the peak [22]. Considering the above experimental results and analysis, it can be concluded that the optimal adsorption time of sulfamethoxazole is 240 min.

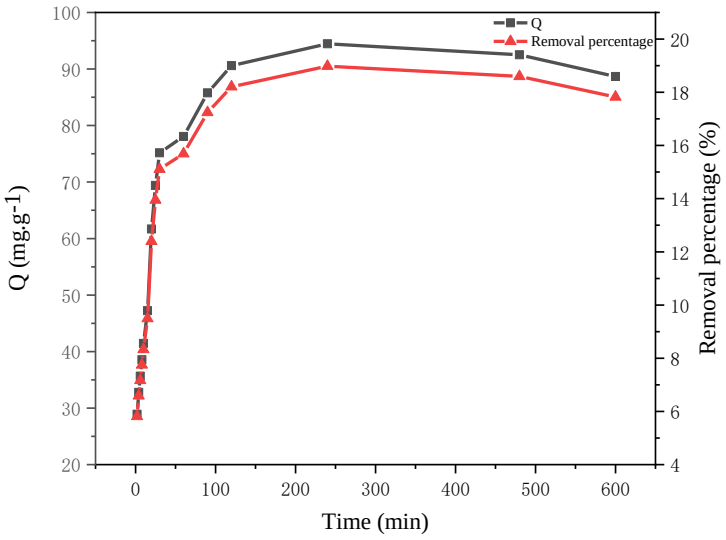

Figure 7. Effect of different time on the adsorption of sulfamethoxazole.

3.4. Effect of different temperatures on the adsorption of sulfamethoxazole

Take 0.010 g 0.4:1, 100 mg·L^{-1}, 480 min at 5 ℃, 15 ℃, 25 ℃, 35 ℃, and 45 ℃. To determine the optimal adsorption temperature. According to the information

shown in **Figure 8**, it can be observed that in 15 ℃ to 35 ℃ range, the adsorption amount and removal efficiency of sulfamethoxazole with temperature, showing obvious upward trend, and peaked at 35 ℃, the adsorption amount and removal rate are: 77.74 $mg \cdot g^{-1}$, 22% respectively, when the temperature exceeds 35 ℃, as the temperature increases further, the adsorption amount and removal rate decreased instead. Therefore, the comprehensive analysis determined that 35 ℃ was the most ideal operating temperature for adsorption.

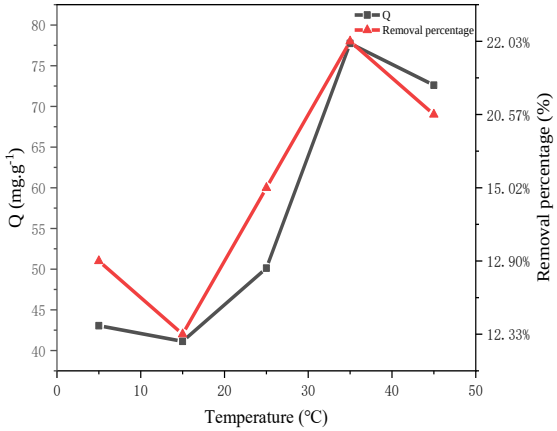

Figure 8. Effect of different temperatures on the adsorption of sulfamethoxazole.

3.5. Effect of different dosage on the adsorption of sulfamethoxazole

To explore the optimal activated carbon injection, the activated carbon samples with a mass ratio of 0.4:1 were selected, which were 0.005 g, 0.010 g, 0.015 g, 0.020 g, and 0.025 g with an initial concentration of 100 $mg \cdot L^{-1}$. The absorbance at each injection volume was measured after 480 min of shaking in a full temperature shaker at 35 ℃. It is found that with the increase of activated carbon addition, the adsorption capacity of sulfamethoxazole showed a decreasing trend, while the removal efficiency increased with longer time. This phenomenon shows that the activated carbon can show the superior adsorption and removal efficiency of sulfamethoxazole. After reviewing the experimental data and weighing various factors, this study recommended using 0.015 g as the optimal activated carbon dose (**Figure 9**).

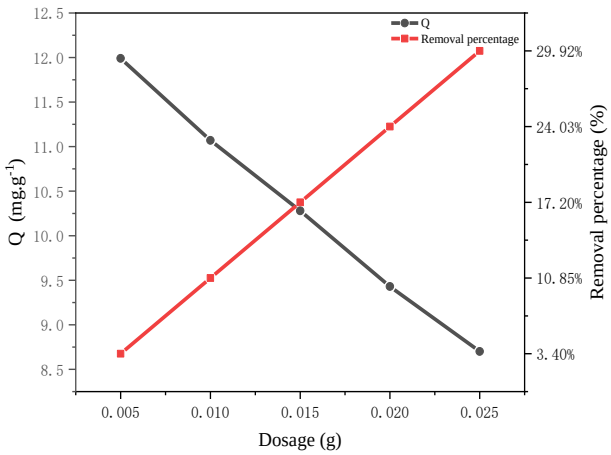

Figure 9. Effect of different dosages on the adsorption of sulfamethoxazole.

3.6. Orthogonal experiment

3.6.1. Range analysis

According to the data analysis in **Table 2**, the adsorption effect was best when the adsorbent dosage was 0.015 g, the initial mass concentration of sulfamethoxazole was 100 mg·L^{-1}, the adsorption time was 240 min, and the adsorption temperature was 35 ℃. This indicates that the adsorption of sulfamethoxazole was maximized under these conditions

Table 2. Orthogonal experimental design table and experimental results.

Experimental number	A Initial concentration (mg·L^{-1})	B Adsorption time (min)	C Investment and quantity (mg)	D The adsorption temperature (℃)	Q_e (mg·g^{-1})
1	80	200	10	25	60.72
2	80	240	15	35	61.04
3	80	280	20	45	52.53
4	100	200	10	25	59.11
5	100	240	15	35	54.94
6	100	280	20	45	54.94
7	120	200	10	25	66.50
8	120	240	15	35	66.82
9	120	280	20	45	63.61
K_1	59.10	62.11	59.76	60.83	
K_2	56.33	59.86	62.32	60.83	
K_3	65.64	59.10	57.99	58.42	
R	9.31	4.01	4.33	2.41	

Note: K_1, K_2 and K_3 are all the mean, and R is extremely poor.

According to the data shown in **Table 2**, the significant order of the adsorption amount affected by each factor is: the initial concentration, followed by the addition, and the adsorption time. Interestingly, the experimental results show that the adsorption process exhibits minimal sensitivity to temperature changes, implying that temperature is not a key variable regulating the adsorption behavior of sulfamethoxazole in an established experimental environment.

3.6.2. Variance analysis

After an in-depth statistical analysis, **Table 3** clearly shows that the F ratio mostly did not reach the F critical threshold, suggesting that the adsorption effect of sulfamethoxazole was not significant among the range of factors examined.

Table 3. Analysis of variance of adsorption capacity.

Divisor	The deviation is square and	Variance	F compare	F critical value	Significance
Initial concentration/mg·L^{-1}	146.81	2	2.78	4.46	
Adsorption time/min	24.28	2	0.46	4.46	
Investment and quantity/g	28.49	2	0.54	4.46	
The adsorption temperature/℃	11.62	2	0.22	4.46	
Deviation	211.19	8			

3.7. Response surface experiment

Design expert10 the software analyzed the experimental data to establish the regression equation for the adsorption amount of sulfamethoxazole *Y*. $Y = 97.50 + 0.3360A - 0.2682B - 0.5142C + 0.1187A0.0192AC + 0.7862BC - 0.4369A2 - 0.7929B2 - 0.6659C2$ (**Table 4**).

Table 4. Experimental design table and experimental results of response surface.

Experimental number	Factor1 A: Initial concentration $mg \cdot L^{-1}$	Factor2 B: While min	Factor3 C: Investment and quantity g	Responsel Adsorption $mg \cdot g^{-1}$
1	120	200	0.015	96.782
2	100	240	0.015	97.480
3	120	280	0.015	96.434
4	100	280	0.01	95.561
5	100	240	0.015	97.426
6	100	240	0.015	97.324
7	100	200	0.02	94.952
8	100	240	0.015	97.626
9	100	280	0.02	96.037
10	100	240	0.015	97.634
11	120	240	0.02	96.235
12	80	200	0.015	96.347
13	80	240	0.02	95.702
14	80	280	0.015	95.524
15	120	240	0.01	97.234
16	80	240	0.01	96.524
17	100	200	0.01	97.621

As can be seen from the above table (**Table 5**), the initial concentration, time, and dosage of the adsorption of sulfamethoxazole, and the significance changed from large to small as C > A > B. The quadratic interaction BC appeared at a very low *p* value (0.0001). In contrast, the adsorption effect of AB and AC on sulfamethoxazole was quite weak and not obvious.

Table 5. Analysis of variance for regression models.

Source of variance	Quadratic sum	Variance	Mean square	*F*	*P*	Significance
Model	12.02	9	1.34	110.90	< 0.0001	**
A-Initial concentration	0.9032	1	0.9032	64.97	< 0.0001	**
B-Time	0.5757	1	0.5757	47.79	0.0002	**
C-Investment and quantity	2.12	1	2.12	175.62	< 0.0001	**
AB	0.0564	1	0.0564	4.68	0.0672	-
AC	0.0015	1	0.0015	0.1230	0.7361	-

Table 5. (*Continued*).

Source of variance	Quadratic sum	Variance	Mean square	*F*	*P*	Significance
BC	2.47	1	2.47	205.27	< 0.0001	**
A^2	0.8038	1	0.8038	66.72	< 0.0001	**
B^2	2.65	1	2.65	219.75	< 0.0001	**
C^2	1.87	1	1.87	155.00	< 0.0001	**
Residual	0.0843	7	0.0120			
Unplanned item	0.0141	3	0.0047	0.2666	0.8470	-
Pure error	0.0703	4	0.0176			*
Overall error	12.11	16				

Note: ** indicates $p < 0.01$, as significant, * indicates $p < 0.05$ as significant, $p > 0.05$ as non-significant, with-non-significant.

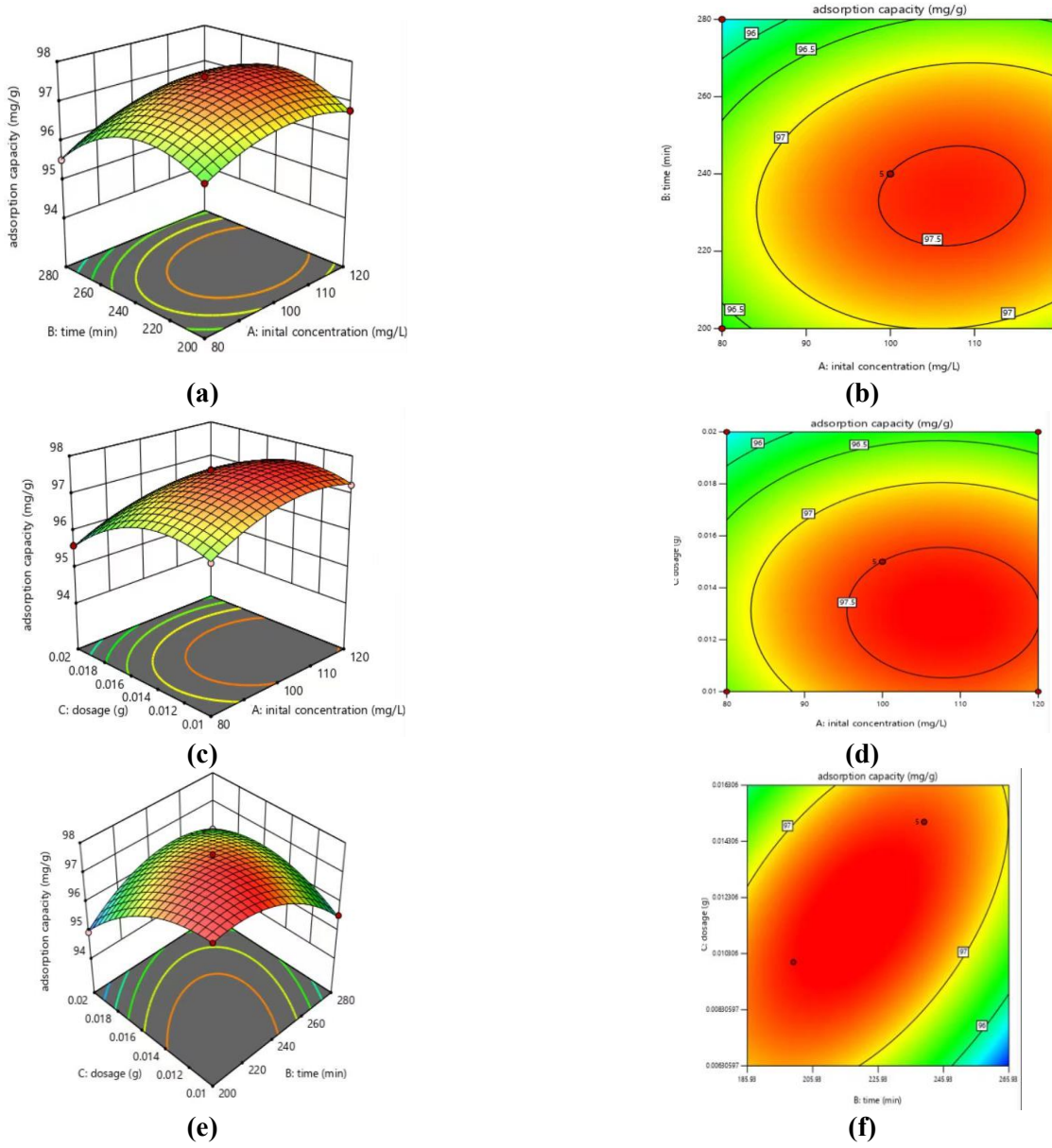

Figure 10. Sulfamethoxazole adsorption response surface analysis.

The slope of the response surface essentially reflects the effect of the interaction on the response value, and the steeper slope often indicates the better fit and predictive power of the model. Therefore, the steepness of the slope should be analyzed to assess the model performance. It is observed that as the concentration rises, the adsorption volume first increases and then decreases, which is clearly shown in the interaction surface diagram of **Figure 10a**. When the initial concentration is low, the adsorption amount is maximum and then reduced. The optimal adsorption amount was achieved when the initial concentration was 120 $mg \cdot L^{-1}$ and the adsorption time was maintained at 240 min. This finding emphasizes that the initial concentration and adsorption time are the two core variables that determine the adsorption efficiency. Through fine regulation of these two parameters, the efficiency of the adsorption process can be greatly improved and the optimal adsorption state can be achieved. **Figure 10b** in the phase response surface, the change from green to red indicates that the response value increases successively, indicating a significant interaction between the two different elements. Moreover, the contour line presenting an elliptical morphology further verified the superiority of this interaction. **Figure 10c** shows that the initial concentration decreases, similarly, the increase of adsorption decreases. The study points out that when the adsorption amount is 0.015 g, the adsorption amount can be maximized, and it is revealed that the initial concentration has a more important influence on the adsorption effect than the adsorption amount. As can be seen in **Figure 10d**, the gradual change from green to red and the response value from small trends, and the interaction between the two factors is obvious. As shown in **Figure 10e**, the dynamics of the adsorption amount first increases and then decreases with the extension of time, and the decrease with the increase of the dose show a more significant effect of the time change on the adsorption amount, thus inferred that the adsorption process is mainly dominated by time variables. **Figure 10f** shows the increasing trend of the response value from outward to inside and the distribution characteristics of the oval, which again confirm the good interaction effect between the two factors.

3.8. Sorption kinetics

Figure 11 presents the fitting scenario of the quasi-first-order and quasi-second-order kinetic models of sulfamethoxazole during the adsorption of activated carbon from biomass sources. It is obvious that, shown graphically (**Table 6**), the fitness index of the quasi-second-order dynamics model is R^2 = 0.9931, which is a significant improvement over R^2 = 0.9070 of the quasi-first-order dynamics. The results strongly imply that the experimental data are more compatible with the quasi-secondary kinetic model, meaning that the adsorption is more likely to involve a chemical adsorption mechanism, beyond the scope of pure physical adsorption. This conclusion further confirms the efficient adsorption capacity of biomass activated carbon for sulfamethoxazole and the main mechanism of chemisorption.

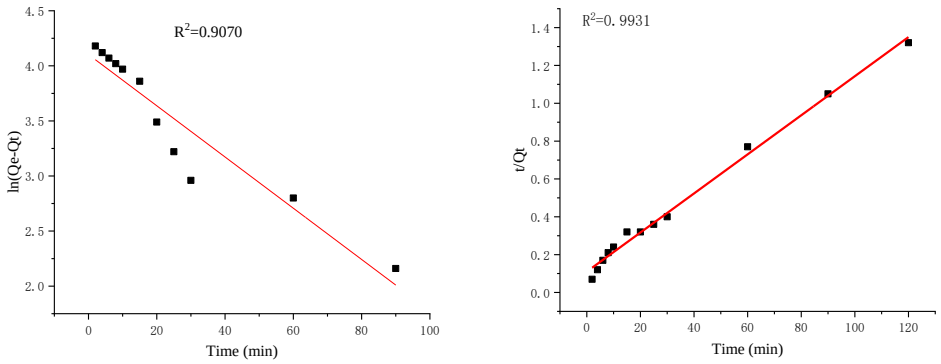

(a) **(b)**

Figure 11. Quasi-primary and quasi-secondary dynamics.

Table 6. Fitting results of adsorption kinetics.

Qexp	Quasi-first-order kinetic parameters			Quasi-second-order kinetic parameters		
	$K_1/(min^{-1})$	qe/(mg·g^{-1})	R^2	$K_2/(min^{-1})$	qe/(mg·g^{-1})	R^2
94.45	0.02325	60.50	0.9070	0.00097	96.81	0.9931

3.9. The adsorption thermodynamics

Figure 12 shows the matching degree of biomass activated carbon for Langmuir and Freundlich adsorption isotherm model during the adsorption process of sulfamethoxazole solution. As can be seen in the Fig, the Freundlich thermodynamic parameter R^2 = 0.6037 is larger than the Langmuir thermodynamic parameter R^2 = 0.59987, therefore, the sulfamethoxazole is better by the Freundlich model. (**Table 7**)

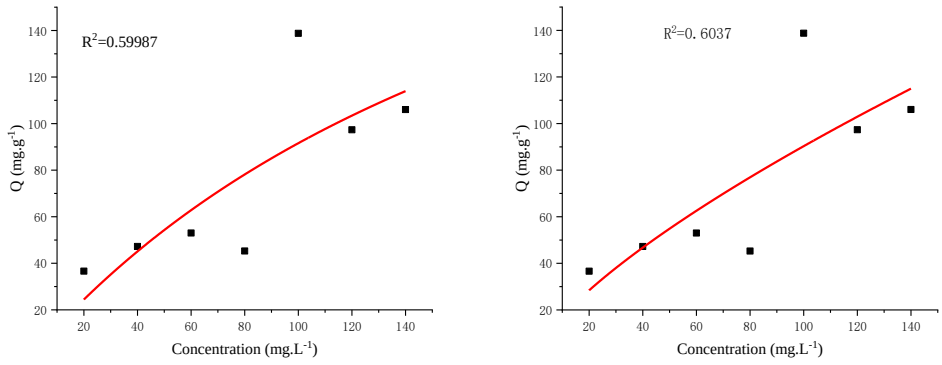

(a) **(b)**

Figure 12. Langmuir adsorption isothermal equation and Freundlich adsorption isothermal equation.

Table 7. The isothermal adsorption model fits the relevant parameters.

Langmuirthermodynamic parameter			Freundlichthermodynamic parameter		
Qm	***K_L***	***R^2***	***K_F***	***1/n***	***R^2***
(mg·g^{-1})	(L·mg^{-1})		(mg·g^{-1})(L·mg)n^{-1}		
292.8393	219.7706	0.59987	3.30096	0.7185	0.6037

4. Conclusion

With the aim of exploring the adsorption efficiency of sulfambuxazole in wastewater. During the study, the rice husk-based biomass char was pretreated, and the separate effects of different operating conditions-initial concentration, time, dosage and temperature were systematically investigated, and the data were analyzed by orthogonal and response surface experiments. The experiment found that rice husk charcoal can effectively adsorb sulfamethoxazole in wastewater, providing a new strategy for wastewater treatment. The main conclusions are drawn from the following points:

(1) SEM test and analysis of cobalt acetate was successfully doped in the biochar interior, and the biochar pore size is uniform, with good adsorption performance. Under the ratio of cobalt acetate to carbon of 0.4:1, the adsorption efficiency of sulfamethoxazole reached the maximum optimization state.

(2) Thermal weight curve analysis the cobalt acetate doped material has better heat resistance, and its stability is better than the original KC biochar.

(3) Under optimal conditions, the adsorption parameters of sulbuxazole by sulbuxazole are: concentration 100 $mg \cdot g^{-1}$, time 240 min, dosage 0.015 g, and temperature 35 ℃.

(4) The adsorption process of sulfamethoxazole solution by biomass activated carbon follows the quasi-secondary kinetic model, and this adsorption characteristic is classified in the category of chemical adsorption.

(5) After in-depth exploration of orthogonal and response surface experiments, we found that the significant degree of influencing factors was different, and the initial concentration and injection amount are the key points.

Author contributions: Conceptualization, ZL and XL (Xinyu Lu); methodology, ZL; software, JK; validation, ZL, JK and XL (Xinyu Lu); formal analysis, JK; investigation, ZL; resources, XL (Xinyu Lu); data curation, JK; writing—original draft preparation, ZL; writing—review and editing, ZL; visualization, XL (Xiaomin Li); supervision, XL (Xiaomin Li); project administration, XL (Xiaomin Li); funding acquisition, XL (Xiaomin Li). All authors have read and agreed to the published version of the manuscript.

Funding: This research was funded by preparation of straw activated carbon and antibiotic adsorption research grant number 2022HJZD01.

Ethical approval: Not applicable.

Conflict of interest: The authors declare no conflict of interest.

References

1. Fan Fang-fang, Tong Zhong-kai, Zuo Wei-yuan. Adsorption of tetracycline from wastewater by calci-modified peanut shell biochar. Inorganicchemicalsindustry, 2023, 55(6):109-115.
2. Xiong Qing-yue, Han Zhi-yong, WU Jie, et al. Adsorption of tetracycline by modified peanut shell biochar. Chemical and Biological Engineering, 2023, 40(3):49-57.
3. Lin Bing-feng, Chen Zhi-hao, Yang Fang-li, et al. Adsorption of tetracycline by manganic-ferrite modified biochar. Journal of Agro-Environmental Science, 2023, 42(7):1585-1596.

4. Messaoudi N E, Khomri M E, Ablouh E ,et al.Biosynthesis of SiO2 nanoparticles using extract of Nerium oleander leaves for the removal of tetracycline antibiotic. Chemosphere, 2022, 287(Pt 4):132453.
5. Liu Ming-kai, Liu Ying-ya, Bao Dan-dan, et al.Effective Removal of Tetracycline Antibiotics from Water using Hybrid Carbon Membranes. Scientific Reports, 2017, 7:43717.
6. Wang Zhe, Wang Guang-jin, Li Wen-yao, et al.Loofah activated carbon with hierarchical structures for high-efficiency adsorption of multi-level antibiotic pollutants.Applied Surface Science, 2021, 550:149313.
7. Lian Xiang, Li Jia-zuo, Wen Guang-lie et al. Research progress of tetracycline removal in water . Modern Rural Science and Technology, 2023, (02):73-74.
8. Shi Liu-min. Study on adsorption of nitroimidazole antibiotics by buckwheat peel biochar . Xi'an University of Technology, 2022.
9. Wang Jia-hao. Study on degradation of tetracycline antibiotics in water by modified biochar activated persulfate . Nanjing Forestry University, 2022.
10. Zeng Cheng, Zheng Huidong, Xu Yibin, et al. Preparation and modification of biomass char and its application in tail water treatment in aquaculture . Fisheries Research, 2024,46 (02): 198-206.
11. Pu Liwei, Mo Lihuan, Hu Yin, et al. K2CO3 Preparation and characterization of activated carbon by activation method . Forest Products Chemistry and Industry, 2024,44 (02): 87-93.
12. Xiong Qingyan month. Preparation modification of peanut shell biochar and its adsorption properties to typical antibiotics in water . Lanzhou University of Technology, 2023.04.
13. Chen Zhihui, Jiang Jie, Sun Guoxin. Advances in the source and removal techniques of sulfonamide antibiotics . Environmental Engineering, 2023,41 (S1): 80-86 + 130.
14. Chen Yongliang, Li Huimin, Shi Lei, et al. Adsorption of amoxicillin by sludge-rice-husk particle biochar in water . Water treatment technology, 2023,49 (10): 64-69.
15. Herrera K, Morales L F, Tarazona N A, et al. Use of biochar from rice husk pyrolysis: part A: recovery as an adsorbent in the removal of emerging compounds. ACS Omega,2022,7(9):7625–7637.
16. Lou J Q, Xu X, Gao Y F, et al. Preparation of magnetic activated carbon from waste rice husk for the determination of tetracycline antibiotics in water samples.RSC Advances,2016,6(113):112166–112174.
17. Shi Juan. Research on the modification of Hanzhong rice husk activated carbon and sulfonamide antibiotics in adsorption water . Grain and Greats, 2022,35 (04): 94-99.
18. Andrade J D L , Moreira C A , Oliveira A G ,et al.Rice Husk-Derived Mesoporous Silica as a Promising Platform for Chemotherapeutic Drug Delivery.Waste and biomass valorization, 2022(1):13.
19. Xiao Huan, Shi Gui-bin, Fang Meng-meng et al. Chinese Journal of Materials Science and Engineering, 2022, 40 (02): 205-210.
20. Wei Cun, Lv Hao-hao, Wang Yu-ying, et al. Adsorption effect of iron-modified rice husk biochar on ammonium nitrogen . Plant Nutrition and Fertilizer Journal, 2021, 27 (04): 595-609.
21. Song Ming. Study on zinc adsorption characteristics of rice husk carbon modified by different methods. Nanjing Agricultural University, 2019.
22. Shi Jia. Study on modification of activated carbon from rice husk and adsorption of sulfonamides in water. Food and Oil, 2022, 35 (04): 94-99.